Applied Mathematics and Computation 216 (2010) 3747–3753

Contents lists available at ScienceDirect

Applied Mathematics and Computation

journal homepage: www.elsevier.com/locate/amc

Fixed-point iterations in determining a Tikhonov regularization parameter in Kirsch's factorization method

Koung Hee Leem [a], George Pelekanos [a,1], Fermín S. Viloche Bazán [b,*,2]

[a] Department of Mathematics and Statistics, Southern Illinois University, Edwardsville, IL 62026, USA
[b] Department of Mathematics, Federal University of Santa Catarina, Florianopolis SC, Santa Catarina, CEP 88040-900, Brazil

ARTICLE INFO

Keywords:
Inverse scattering problems
Kirch's factorization method
Tikhonov regularization
L-curve criterion

ABSTRACT

Kirsch's factorization method is a fast inversion technique for visualizing the profile of a scatterer from measurements of the far-field pattern. The mathematical basis of this method is given by the far-field equation, which is a Fredholm integral equation of the first kind in which the data function is a known analytic function and the integral kernel is the measured (and therefore noisy) far-field pattern. We present a Tikhonov parameter choice approach based on a fast fixed-point iteration method which constructs a regularization parameter associated with the corner of the L-curve in log–log scale. The performance of the method is evaluated by comparing our reconstructions with those obtained via the L-curve and we conclude that our method yields reliable reconstructions at a lower computational cost.

1. Introduction

For inverse acoustic scattering the original linear sampling method was introduced by Colton and Kirsch [1], and mathematically clarified in [2]. Kirsch [3] improved the original version of the linear sampling method, leading to the so-called $(F^{\star}F)^{1/4}$-method. Recently, Arens [4] presented a proof of convergence for this method for the case of acoustic scattering by sound soft obstacles. Linear sampling methods involve the solution of a linear Fredholm equation of the first kind, the far-field equation, which is written for each point x_0 inside the scatterer and whose integral kernel is the far-field pattern, i.e. far-field data that are usually contaminated with significant noise. Its right-hand side is an exactly known analytic function. In particular, linear sampling methods attempt to recover the object by sampling the space by using functions that take known value when they are evaluated inside the object. Consequently, in the second version of the linear sampling method, Kirsch, characterized the obstacle in terms of the spectral data of the far-field operator F. Two of the attractive futures of this method is its computational speed, and the very low amount of *a priori* information of the physical properties of the scatterers. One of its disadvantages though is that it only gives an explicit characterization of the scattering obstacle (i.e. it only determines the support of the scatterer).

It is well known that every numerical implementation of an inverse scattering method requires at some point regularization in order to cope with the ill-posedness of the problem, and the linear sampling method is not an exception. In most numerical applications of the linear sampling method, Tikhonov regularization has been employed and the regularization constant was computed via Morozov's discrepancy principle [2], which involved the computation of the zeros of the

* Corresponding author.
E-mail addresses: kleem@siue.edu (K.H. Leem), gpeleka@siue.edu (G. Pelekanos), fermin@mtm.ufsc.br (F.S.V. Bazán).
[1] This research was supported by the Hoppe Professorship Award, Southern Illinois University, Edwardsville.
[2] This research was sponsored by CNPq, Brazil, Grant 308154/2008-8.

0096-3003/$ - see front matter © 2010 Elsevier Inc. All rights reserved.
doi:10.1016/j.amc.2010.05.036

discrepancy function at each point of the grid, a process that is time-consuming. In addition, the noise level in the data should be known *a priori*, something that in real life applications is not the case in general. Several other strategies for selecting the regularization parameter have been proposed, one of them being the L-curve method [5], see also [6] for an application of the L-curve method in inverse elastic scattering. The L-curve method is a log–log plot of the norm of a regularized solution versus the norm of the corresponding residual norm. It relies on the observation that the vertical part of the curve for small changes in the regularization parameter corresponds to rapidly varying regularized solutions with very little change in the residual norm, while the horizontal part for large values of the regularized parameter corresponds to slowly varying regularized solutions with large changes in the residual norm. Hence, a reasonable regularized solution should lie in the vicinity of the 'corner' of the L-curve. The L-curve method selects the parameter which maximizes the curvature of the L-curve. However, computing the point of maximum curvature in a robust way is not an easy task [5,7,8].

In this work we propose a fixed-point (FP) algorithm for selecting the regularization parameter based on an earlier work of Reginska [8] and Bazán [9,10], which we use for the characterization of an object via Kirsch's $(F^{\star}F)^{1/4}$ -method. The FP algorithm only needs computation of the solution norm (or solution seminorm) and the residual norm, while the L-curve requires either the SVD (or GSVD) or the computation of the derivative of the solution norm with respect to the regularization parameter. Hence the FP algorithm is simpler and better suited for large-scale problems.

In what follows the method will be denoted by MKM-FP which stands for modified Kirsch's method coupled with the FP-algorithm.

We organize our paper as follows. Section 2 will be devoted to the formulation of the problem and a brief description of the Kirsch's factorization method. Consequently, Section 3 will deal with the description of the FP algorithm as a parameter choice method. In Section 4, we will be concerned with the idea behind the selection of our parameter as well as with its implementation within the framework of the linear sampling method. In order to show the effectiveness of our approach we will present numerical examples for the case of inpenetrable scatterers. For the reconstructions we will use simulated data obtained by means of the Nyström method [11]. We will finally list our conclusions in Section 5.

2. A description of the factorization method

It is well known that the propagation of time-harmonic acoustic fields in a homogeneous medium, in the presence of a sound soft obstacle D, is modeled by the exterior boundary value problem (direct obstacle scattering problem)

$$\triangle_2 u(x) + k^2 u(x) = 0, \quad x \in \mathbb{R}^2 \setminus \overline{D}, \tag{2.1}$$

$$u(x) + u^i(x) = 0, \quad x \in \partial D, \tag{2.2}$$

where k is a real positive wavenumber and u^i is a given incident field, that in the presence of D will generate the scattered field u.

In addition, the scattered field u will satisfy the Sommerfeld radiation condition

$$\lim_{r\to\infty} \sqrt{r}\left(\frac{\partial u}{\partial r} - iku\right) = 0, \tag{2.3}$$

$|r| = |x|,\ x \in \mathbb{R}^2 \setminus \overline{D}$, and the limit is taken uniformly for all directions $\hat{x} = x/|x|$.

The Green formula implies that the solution u of the direct obstacle scattering problem above has the asymptotic behavior

$$u(x) = u_\infty(\hat{x})\frac{e^{ikr}}{\sqrt{r}} + O(r^{-3/2}) \tag{2.4}$$

for some analytic function u_∞, called the far-field-pattern of u, and defined on the unit sphere Ω. In the case of the inverse problem, it represents the measured data. In particular, the inverse problem that will be considered here, is the problem of finding the shape of D from a complete knowledge of the far-field pattern.

We now define the far-field equation

$$(Fg_z)(\hat{x}) = \frac{e^{i\pi/4}}{\sqrt{8\pi k}} e^{-ik\hat{x}\cdot z}, \tag{2.5}$$

where the right-hand side is the far-field pattern of the fundamental solution of the Helmholtz equation, $z \in \mathbb{R}^2$ and $F{:}L^2(\Omega) \to L^2(\Omega)$ is given by

$$(Fg)(\hat{x}) = \int_\Omega u_\infty(\hat{x};\hat{d})g(\hat{d})ds(\hat{d}), \quad d \in \Omega \tag{2.6}$$

It is well known that the first version of the linear sampling method [1] solves the linear operator equation (2.5) based on the numerical observation that its solution will have a large norm outside and close to ∂D. Hence, reconstructions are obtained by plotting the norm of the solution. However, the problem is that the right-hand side does not in general belong to the range of the operator F. Kirsch [3] was able to overcome this difficulty with the introduction of a new version of the linear sampling method based on appropriate factorization of the far-field operator F. In this method, Kirsch is elegantly using the spectral

properties of the operator F to characterize the obstacle. In particular, the following far-field equation is now used in place of Eq. (2.5)

$$(F^{\star}F)^{1/4}g_z = \frac{e^{i\pi/4}}{\sqrt{8\pi k}}e^{-ik\hat{x}\cdot z} \tag{2.7}$$

and the spectral properties of F are used for the reconstructions. However, due to noisy data, the discretized version of the far-field operator F is characterized by numerical instability which may result to false information about its singular system. In the next section, we will show that we can overcome this difficulty via the a priory determination of a Tikhonov regularization parameter.

3. The fixed-point method for the selection of the Tikhonov parameter

We start by introducing appropriate notation concerning Tikhonov's method for problems of the form

$$\min_{f\in\mathbb{R}^n}\|b - Af\|_2, \quad A \in \mathbb{R}^{k\times n}(k \geqslant n), \quad b \in \mathbb{R}^k, \tag{3.8}$$

where A is ill-conditioned and has singular values decaying to zero without particular gap in the singular value spectrum. In its simplest form, Tikhonov's method amounts to replacing the least squares problem (3.8) by

$$\min_{f\in\mathbb{R}^n}\{\|b - Af\|_2^2 + \lambda^2\|f\|_2^2\}, \tag{3.9}$$

where $\lambda > 0$ is the regularization parameter. Solving (3.9) is equivalent to solving the *regularized* normal equations

$$(A^TA + \lambda^2 I_n)f = A^Tb, \tag{3.10}$$

whose solution is $f_\lambda = (A^TA + \lambda^2 I_n)^{-1}A^Tb$, where I_n is the $n \times n$ identity matrix.

Let the SVD of A be

$$A = U\Sigma V^*,$$

where U and V are square orthonormal matrices, and $\Sigma = \mathrm{diag}(\sigma_1,\ldots,\sigma_n)$, with $\sigma_1 \geqslant \sigma_2 \cdots \geqslant \sigma_p > \sigma_{p+1} = \cdots = 0$, $p = \mathrm{rank}(A) \leqslant n$.

Define $\alpha_i = |u_i^Tb|^2$ (the squared Fourier coefficient of b), and $\delta_0 = \|(I - UU^T)b\|_2$ (the size of the incompatible component of b that lies outside the column space of A).

Define also $y(\lambda) = \|f_\lambda\|_2^2$, and $x(\lambda) = \|b - Af_\lambda\|_2^2$. Then it is easy to see that

$$x(\lambda) = \sum_{i=1}^{p}\frac{\lambda^4\alpha_i}{(\sigma_i^2+\lambda^2)^2} + \delta_0^2, \quad y(\lambda) = \sum_{i=1}^{p}\frac{\sigma_i^2\alpha_i}{(\sigma_i^2+\lambda^2)^2}. \tag{3.11}$$

The fixed-point method can be regarded as a realization of a parameter choice rule devised by Regińska [8], who proposed as regularization parameter a local minimum of the function

$$\Psi_\mu(\lambda) = x(\lambda)y^\mu(\lambda), \tag{3.12}$$

for proper $\mu > 0$. The motivation for using this rule can be supported heuristically noting that when λ is small, the squared solution norm $y(\lambda)$ gets large while $x(\lambda)$ gets small, and $\Psi_\mu(\lambda)$ is not minimized. Conversely, when λ is large, $y(\lambda)$ gets small while $x(\lambda)$ gets large, and once again $\Psi_\mu(\lambda)$ is not minimized. This suggests that the minimizer of $\Psi_\mu(\lambda)$ corresponds to a good balance between the size of the solution norm and the size of the corresponding residual norm. Regińska proved that if the curvature of the L-curve is maximized at $\lambda = \lambda^*$, and if the tangent to the L-curve at $(\log x(\lambda^*), \log y(\lambda^*))$ has slope $-1/\mu$, then $\Psi_\mu(\lambda)$ is minimized at $\lambda = \lambda^*$.

Bazán [9] investigated the properties of $\Psi_\mu(\lambda)$ and concluded that its minimizers are converging values of a sequence defined by

$$\lambda_{j+1} = \phi_\mu(\lambda_j), \quad j \geqslant 0, \quad \phi_\mu(\lambda) = \sqrt{\mu}\frac{\|b - Af_\lambda\|_2}{\|f_\lambda\|_2}, \quad \lambda > 0, \tag{3.13}$$

which gave rise to the fixed-point (FP) algorithm. One of the main advantages of the FP method is that it does not exploit any knowledge of the norm of the error in g. The main steps of FP can be described as follows:

- Given a proper initial guess, FP starts with $\mu = 1$ as a default value, and then proceeds with the iterates (3.13) until the largest convex fixed-point of ϕ_1 is reached (a convex fixed-point is a fixed point of ϕ_1 at which the L-curve is locally convex [10]). The choice $\mu = 1$ is because in most problems this value yields a regularization parameter that leads to a point on the L-curve near the corner of maximum curvature.
- If $\mu = 1$ does not work (which means $\phi_1(\lambda) > \lambda$ for all $\lambda > 0$), μ is adjusted and the iterations restart; see [9,10] for details.

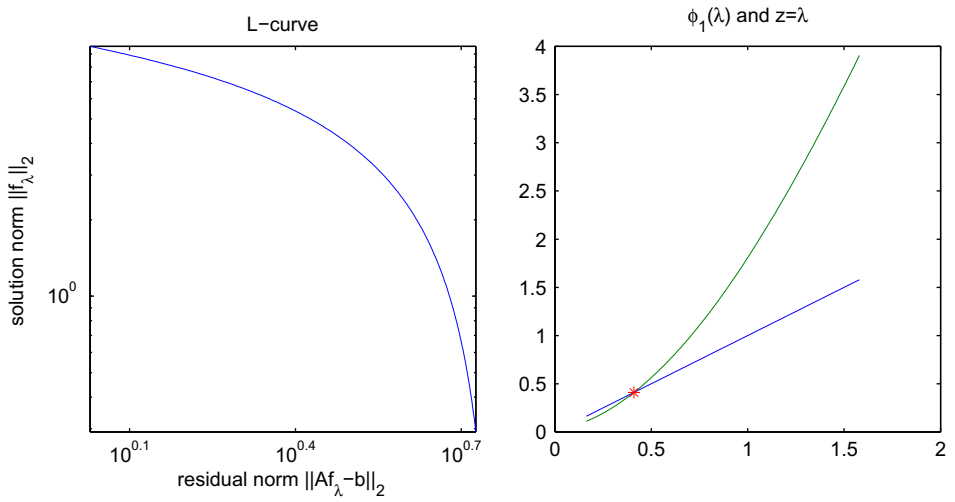

Fig. 1. Concave L-curve in all domain and corresponding curve ϕ_1.

Numerical experiments have shown that FP performs well when the L-curve is well-behaved (i.e., when there is a unique and sharp convex L-corner), and when the convexity regions of the L-curve are well-defined, as often seen in most practical problems.

However, since minimizers of Ψ_μ (when they exist) are points where the L-curve is convex [8,10], it is intuitively clear that the FP should fail when the L-curve is concave for all $\lambda > 0$. Such an example is depicted in Fig. 1. In this example, since the L-curve is concave in the whole domain, the only fixed-point of the function ϕ_1 (see dotted line) *maximizes* Ψ_1 and the FP algorithm fails.

We end this review with some convexity results on the L-curve due to Regińska [8].

- When $\delta_0 \neq 0$ the curve is always convex on $(0,\epsilon)$ for ϵ sufficiently small and concave on (σ_1,∞).
- When $\delta_0 = 0$ the L-curve is concave on $(0,\sigma_n) \cup (\sigma_1,\infty)$. The case $\delta_0 = 0$ is typical of problems where $g \in \mathcal{R}(A)$ and occurs, e.g., when $k = n$ and A is nonsingular.

More informative results on convexity properties of the L-curve can be found in [10].

4. Numerical method and applications

In this section we shall describe a method for selecting the Tikhonov regularization parameter in connection with Kirsch's $(F^*F)^{1/4}$ method [3]. Recall that in practice, the goal of Kirsh's method is to solve a finite dimensional linear equation

$$(\widetilde{F}_d^*\widetilde{F}_d)^{1/4} g = r_z,$$

for each z in the grid and where r_z is given by the right-hand side of Eq. (2.7), $\widetilde{F}_d$ is a perturbed finite-dimensional far-field operator: $\widetilde{F}_d = F_d + E \in \mathbb{C}^{n\times n}$, and n denotes the number of observed incident fields. We also observe that because the far-field operator is compact, the singular values of F_d decay quickly to zero and in general there is no particular gap in the singular spectrum. Taking all these under consideration, the problem we are interested in is to select the Tikhonov regularization parameter for

$$\min_{g\in\mathbb{R}^n}\{\|r_z - \widetilde{A}_d g\|_2^2 + \lambda^2\|g\|_2^2\}, \tag{4.14}$$

where for simplicity we denote $\widetilde{A}_d = (\widetilde{F}_d^*\widetilde{F}_d)^{1/4}$. The choice of λ for the above problem has been done via Morozov's discrepancy principle [1–3], adapted to the case when the data matrix is corrupted by noise. The strategy is reliable but the noise level (or some estimate) must be known in advance. However, the norm of the error $A_d - \widetilde{A}_d$ is rarely available in practice (making the discrepancy principle of little use), and rules that do not exploit this information are highly desirable.

In what follows we will discuss how to choose the Tikhonov regularization parameter by using the FP-method and without requiring any knowledge of the noise level in the far-field matrix.

We start with the crucial observation that since $\widetilde{F}_d$ is square and nonsingular (since A_d so is), the linear system

$$\widetilde{A}_d g = r_z \tag{4.15}$$

is always compatible and hence the important constant δ_0 introduced in the previous section satisfies $\delta_0 = 0$. To make matters worse, numerical examples for several reconstruction problems showed that the iteration function ϕ_1 has a unique fixed

point that is a maximizer of Ψ_1, making the FP-method unpractical for solving the reconstruction problem. In order to overcome this difficulty we propose to replace $\widetilde{A}_d$ by another matrix, say $\widetilde{B}_d$, with $\widetilde{B}_d$ close to A_d in some sense and such that the constant δ_0 associated with $\widetilde{B}_d$ satisfies $\delta_0 \neq 0$. To be precise, let the SVD of $\widetilde{F}_d$ be

$$\widetilde{F}_d = \widetilde{U}\widetilde{\Sigma}\widetilde{V}^* = \sum_{i=1}^{n} \tilde{\sigma}_i \tilde{u}_i \tilde{v}_i^*$$

so that $\widetilde{A}_d = \sum_{i=1}^{n} \sqrt{\tilde{\sigma}_i}\,\tilde{v}_i \tilde{v}_i^*$. Then if we take $\widetilde{B}_d$ to be

$$\widetilde{B}_d = \sum_{i=1}^{m} \sqrt{\tilde{\sigma}_i}\,\tilde{v}_i \tilde{v}_i^*,$$

with a chosen cut-off index $m < n$, our proposal is to reconstruct the object by solving (4.14) with $\widetilde{B}_d$ in place of $\widetilde{A}_d$ and with the Tikhonov parameter being chosen via the FP-method. The motivation for this choice is that the exact far-field matrix F_d always has at least one negligible singular value. In what follows this method will be denoted by MKM-FP which stands for modified Kirsch's method coupled with the FP-algorithm.

In order to explain why MKM-FP is expected to work, we observe that the constant δ_0 associated with matrix $\widetilde{B}_d$ is given by $\delta_0^2 = \sum_{i=m+1}^{n} |\tilde{v}_i^* r_z|^2$ and that this value is expected to be very small but nonzero. A by-product of this is that there exists a vicinity of the origin in which the L-curve is convex and so at least one minimizer of Ψ_1 is always guaranteed to exist [8]. In order to illustrate the fundamental difference of using $\widetilde{B}_d$ instead of $\widetilde{A}_d$, we have computed the functions ϕ_1 and Ψ_1 associated with (2.7) as well as the corresponding functions associated with MKM-FP which we denote by $\phi_1^{(m)}$ and $\Psi_1^{(m)}$ respectively. The problem considered in this illustration is that of reconstructing the profile of a kite. All these functions are depicted in Fig. 2.

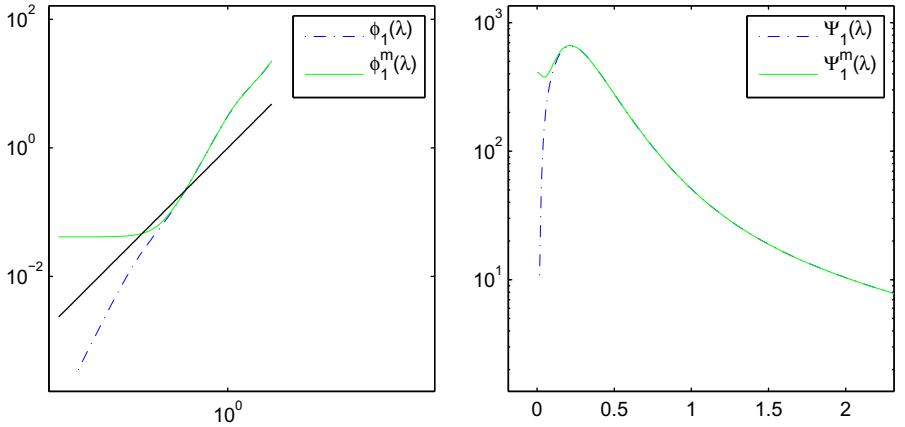

Fig. 2. Functions ϕ_1 and Ψ_1 for the problem (2.7) and functions $\phi_1^{(m)}$ and $\Psi_1^{(m)}$ associated with MKM-FP.

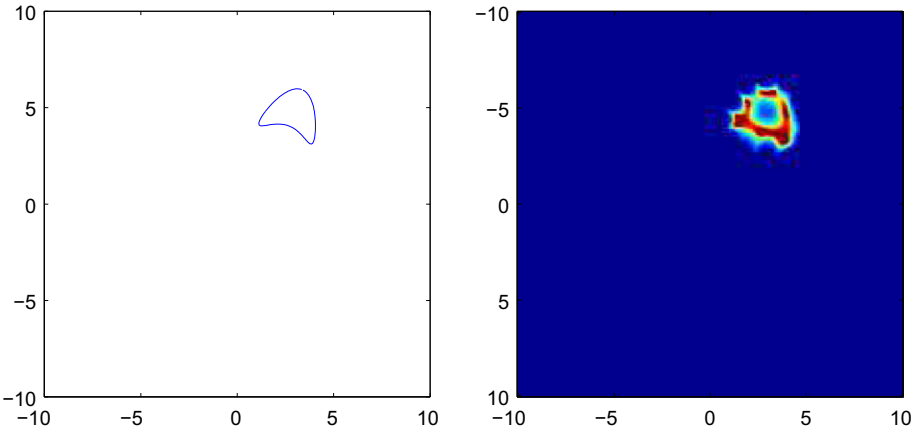

Fig. 3. Profile of a kite and its reconstruction without regularization.

Observe from this figure that while ϕ_1 has a unique fixed-point that maximizes Ψ_1, the function $\phi_1^{(m)}$ has two fixed-points, the smallest one being a minimizer and the largest one being a maximizer of $\Psi_1^{(m)}$.

Note that the cut-off index m is chosen to be the largest index in which the quantity $\sum_{i=m+1}^{n} |\tilde{v}_i^* r_z|^2 < \epsilon$ for a given tolerance ϵ. In our image reconstruction experiments with one object, a tolerance of 1.0e−12 is used.

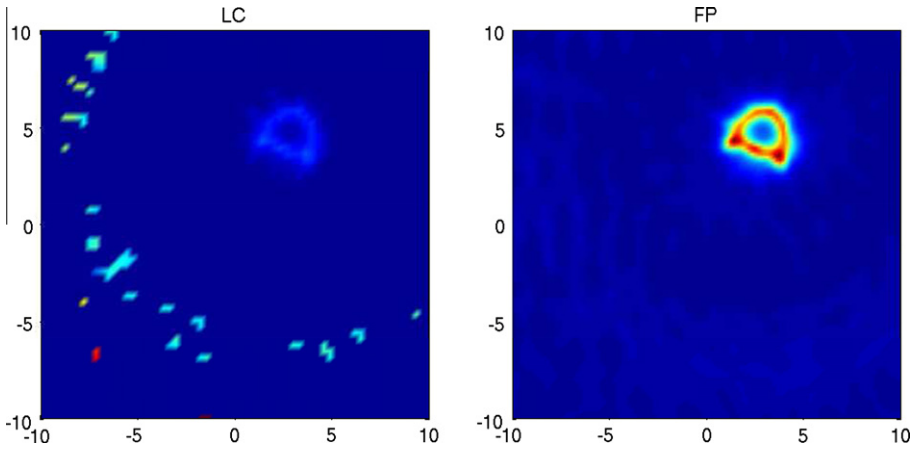

Fig. 4. Reconstruction results using L-curve and FP shown on a grid of 127 × 127 obtained by interpolating the $\|g_z\|_2$ values.

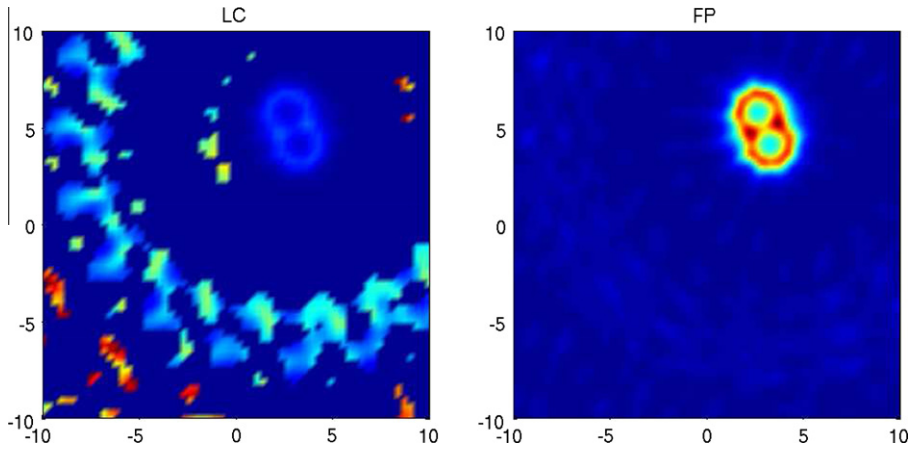

Fig. 5. Reconstruction results using L-curve and FP shown on a grid of 127 × 127 obtained by interpolating the $\|g_z\|_2$ values.

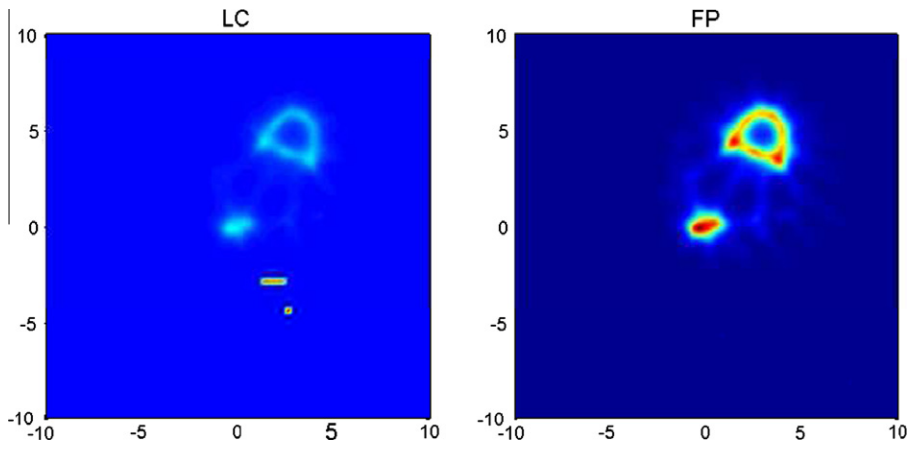

Fig. 6. Reconstruction results using L-curve and FP for a kite and an ellipse shown on a grid of 159 × 159 obtained by interpolating the $\|g_z\|_2$ values.

The profile of the kite and its reconstructed version obtained without regularization are shown in Fig. 3. In this example the far-field matrix $\tilde{F}_d$ is 21×21 (i.e., we use 21 incident observed directions), the noise level (in a relative sense) is 4.3% and the object is located in a grid of 64×64 points.

For MKM-FP, only the first 20 singular values and corresponding singular vectors are used, that is the cut-off index m is 20. The results of MKM-FP are displayed in Fig. 4 where we have also included the results obtained by Kirsch's method where the L-curve criterion is used for the selection of the Tikhonov regularization parameter.

Our second experiment is concerned with the application of MKM-FP method to the reconstruction of the profile of a peanut from 20 incident fields. Here again we use a grid of 64×64 points and a far-field matrix with approximately 2% of noise (in a relative sense). The results of both L-curve and MKM-FP are displayed in Fig. 5. Note that the cut-off index $m = 19$ is used with the same tolerance ϵ.

In our last numerical experiment we reconstruct two objects, a kite and an ellipse, from 50 incident fields. We use a grid of 80×80 and a far-field matrix with approximately 2% of noise. The tolerance ϵ for the cut-off index m is increased to 1.0e−10 due to the larger number of incident fields, and resulted in removing the two smallest singular-value pairs. Reconstructions using both the L-curve and the MKM-FP are displayed in Fig. 6.

5. Conclusions

We proposed a fixed-point algorithm that selects a Tikhonov parameter associated with the characterization of an impenetrable scatterer using Kirsch's factorization method. Numerical results suggest that the MKM-FP's cost is extremely modest (comparing to that of the L-curve) and robust. In addition, our algorithm produces visually satisfactory reconstructions without a-priory knowledge of the noise level, in contrast to the Morozov discrepancy principle that till recently was used by most researchers [1–3]. Future research will be geared towards extending the method to three dimensional problems.

References

[1] D. Colton, A. Kirsch, A simple method for solving the inverse scattering problems in the resonance region, Inverse Problems 12 (1996) 383–393.
[2] D. Colton D, M. Piana, R. Potthast, A simple method using Morozov's discrepancy principle for solving inverse scattering problems, Inverse Problems 13 (1999) 1477–1493.
[3] A. Kirsch, Characterization of the shape of a scattering obstacle using the spectral data of the far field operator, Inverse Problems 14 (1998) 1489–1512.
[4] T. Arens, Why linear sampling works, Inverse Problems 20 (2004) 163–173.
[5] P.C. Hansen, Rank-Deficient and Discrete Ill-Posed Problems, SIAM, Philadelphia, 1998.
[6] G. Pelekanos, V. Sevroglou, Shape reconstruction of a 2D-elastic penetrable object via the L-curve method, Journal of Inverse Ill-Posed Problems 14 (4) (2006) 1–16.
[7] M. Hanke, Limitations of the L-curve method in ill-posed problems, BIT 36 (1996) 287–301.
[8] T. Regińska, A regularization parameter in discrete ill-posed problems, SIAM Journal of Scientific Computing 3 (1996) 740–749.
[9] F.S.V. Bazán, Fixed-point iterations in determining the Tikhonov regularization parameter, Inverse Problems 24 (2008) 1–15.
[10] F.S.V. Bazán, J.B. Francisco, An improved fixed-point algorithm for determining a Tikhonov regularization parameter, Inverse Problems 25 (2009).
[11] D. Colton, R. Kress, Inverse Acoustic and Electromagnetic Scattering Theory, Springer-Verlag, New York, 1992.